ChemComm

Accepted Manuscript

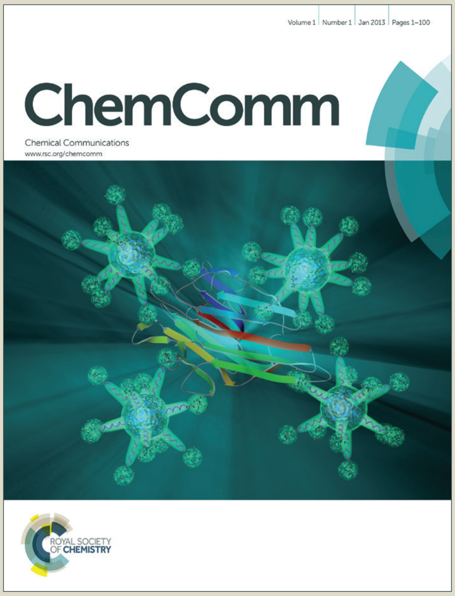

ROYAL SOCIETY OF CHEMISTRY

www.rsc.org/chemcomm

Journal Name RSCPublishing

COMMUNICATION

Cite this: DOI: 10.1039/x0xx00000x

Received 00th January 2014,
Accepted 00th January 2014

DOI: 10.1039/x0xx00000x

www.rsc.org/

One-step synthesis of bismuth molybdate catalysts via flame spray pyrolysis for the selective oxidation of propylene to acrolein

K. Schuh,[a] W. Kleist,[a,b] M. Høj,[c] V. Trouillet,[d] A. D. Jensen[c] and J.-D. Grunwaldt[a,b]

Flame spray pyrolysis (FSP) of Bi(III)- and Mo(VI)-2-ethylhexanoate dissolved in xylene resulted in various nanocrystalline bismuth molybdate phases depending on the Bi/Mo ratio. Besides α-$Bi_2Mo_3O_{12}$ and γ-Bi_2MoO_6, FSP gave direct access to the metastable β-$Bi_2Mo_2O_9$ phase with high surface area (19 m²/g). This phase is normally only obtained at high calcination temperatures (> 560 °C) resulting in lower surface areas. The β-phase was stable up to 400 °C and showed superior catalytic performance compared to α- and γ-phases in selective oxidation of propylene to acrolein at temperatures relevant for industrial applications (360 °C).

Multicomponent mixed oxides (MMO) based on bismuth and molybdenum with addition of iron and cobalt are industrially used as catalysts for selective oxidation of propylene to acrolein for methionine production [1] and as intermediate to acrylic acid [2]. It is generally accepted that bismuth molybdates are located at the catalyst surface providing the key active sites, whereas iron and cobalt molybdates are situated in the bulk. [3, 4] The specific surface area of bulk bismuth molybdates is often rather low (1 – 4 m²/g). [5-10] Addition of other transition metals increases the specific surface area but the surface related activity of these MMOs is only higher in the presence of iron. [11] In order to improve the overall reaction rate it would be beneficial to increase the surface area of bulk bismuth molybdates and compare the catalytic performance of the different crystalline phases, i.e. α-$Bi_2Mo_3O_{12}$, β-$Bi_2Mo_2O_9$ and γ-Bi_2MoO_6. Beale and Sankar [12] prepared bismuth molybdates by hydrothermal synthesis at different pH values resulting in surface areas of 8 – 10 m²/g for the as-prepared materials. Calcination at 400 °C did not decrease the surface area significantly, whereas calcination at 560 °C resulted in extensive sintering. Le et al. used spray drying [7, 13] and complexation [13] for the preparation of α-, β- and γ-bismuth molybdate. Addition of citric acid during spray drying increased the surface area to a maximum of 12 m²/g for α-$Bi_2Mo_3O_{12}$ and supplementary variation of the pH value resulted in a surface area up to 17 m²/g for γ-Bi_2MoO_6. This increase in surface area also improved the rate of acrolein formation. Nell et al. [14] applied a templating approach for the synthesis of high surface area bismuth molybdates and bismuth vanadates for selective propylene oxidation. They used mesoporous silica and carbons as templates for the preparation of $Bi_2Mo_3O_{12}$.

The bismuth molybdate phases relevant for selective oxidation of propylene to acrolein are α-$Bi_2Mo_3O_{12}$, metastable β-$Bi_2Mo_2O_9$ and γ-Bi_2MoO_6 but despite intensive research, there is still a debate in the literature about the relative activity of these bismuth molybdate phases. As outlined above, a number of preparation methods such as co-precipitation [5, 6, 15], solid state reaction [16] and spray drying [7, 13] have been applied under different preparation conditions. In all cases only higher calcination temperatures led to the formation of β-bismuth molybdate, which is in line with the phase diagram established by Egashira et al. [17] showing that β-$Bi_2Mo_2O_9$ only forms above 540 °C. In fact, Beale and Sankar [12] treated their samples at 400 °C to obtain α- and γ-bismuth molybdate, but required 560 °C to produce the β-phase. Le et al. [13] calcined the as-prepared materials at 500 °C, 550 °C and 600 °C resulting in α-, γ- and β-bismuth molybdate, respectively. However, the higher calcination temperatures led to a lower surface area, which we also found in a previous study. [18]

Hence, a method is required that provides temperatures > 540 °C and at the same time does not result in particle sintering. Potentially, flame spray pyrolysis (FSP) is suited for this purpose. This novel synthesis method uses high preparation temperatures (up to 3000 K) [19] but very short residence time (~1 ms). [20, 21] We report in this communication that this one-step method allows the preparation of α-, β- and γ-bismuth molybdate under similar synthesis conditions by just varying the initial Bi/Mo ratio. The three materials were then tested in the selective oxidation of propylene to acrolein.

For the flame synthesis, Bi(III)- and Mo(VI)-2-ethylhexanoate were dissolved in xylene to a total metal concentration of 0.15 mol/l at Bi/Mo ratios of 2:1, 1:1 and 2:3 resulting in the corresponding bismuth molybdate phase (γ-Bi_2MoO_6, β-$Bi_2Mo_2O_9$, α-$Bi_2Mo_3O_{12}$). The solutions were sprayed using oxygen as dispersion gas and ignited by a methane/oxygen flame with a recently established set-up at KIT based on previous designs by Mädler and Pratsinis [22-24]. A detailed description of the preparation is given in the Electronic Supporting Information (ESI †). The obtained bismuth molybdate samples were characterized by powder X-ray diffraction (PXRD), nitrogen physisorption, X-ray absorption spectroscopy (XAS), optical emission spectrometry with inductively coupled plasma (ICP-OES), transmission electron microscopy (TEM) and X-ray photoelectron spectroscopy (XPS); the results are given in Fig. 1 and Table 1 (additional data cf. ESI †).

The diffraction patterns of the samples synthesized with Bi/Mo = 2:1 and Bi/Mo = 1:1 (cf. Fig. 1) show well-defined reflections of high intensity at 2θ = 28.2 ° and 27.8 ° which is in good agreement with the diffraction patterns of γ-Bi_2MoO_6 and β-$Bi_2Mo_2O_9$, respectively. The flame made material synthesized with Bi/Mo = 2:3 was highly amorphous and only exhibited one small reflection at 2θ = 27.9 ° matching the main reflection of α-$Bi_2Mo_3O_{12}$. The ratio of bismuth to molybdenum in the bulk determined by ICP-OES corresponded to the applied ratio for the sample synthesized with Bi/Mo = 2:1 (see Table 1) indicating that the precursors were completely transformed. For γ-Bi_2MoO_6 synthesized with Bi/Mo = 2:1 an excess of bismuth was detected at the surface by XPS (cf. Table 1). The surface composition of the catalysts was calculated using the peak areas of Mo $3d_{5/2}$ = 232.7 eV and Bi $4f_{7/2}$ = 159.4 eV in the XPS indicating the presence of Bi^{3+} and Mo^{6+}.[25] High Bi/Mo surface ratios were also reported in the literature for γ-Bi_2MoO_6 prepared by different methods (spray dried: 2.4 [7], co-precipitated: 2.6 [6]). The sample synthesized with Bi/Mo = 1:1 composed of β-$Bi_2Mo_2O_9$ resulted in a Bi/Mo ratio on the surface of 1.1 which agrees well with the results reported for β-$Bi_2Mo_2O_9$ by Matsuura et al. [9] and Soares et al. [26].

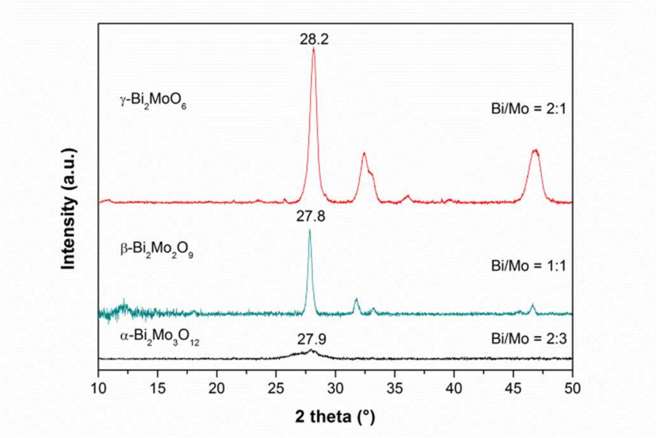

Fig. 1 X-ray diffraction patterns of samples synthesized by flame spray pyrolysis with three different Bi/Mo ratios resulting in three different phases.

Table 1 Phase composition, specific surface area and ratio of bismuth to molybdenum on the surface as well as maximum acrolein yield obtained in catalytic activity measurements.

Applied Bi/Mo ratio	Phase according to PXRD	Specific surface area (BET) (m²/g)	Surface Bi/Mo ratio [a] (at.%/at.%)	Max. acrolein yield at 360 °C [c] (%)
2:1	γ-Bi_2MoO_6	45	2.3 [b]	11.2
1:1	β-$Bi_2Mo_2O_9$	19	1.1	18.8
2:3	α-$Bi_2Mo_3O_{12}$	18	-	3.4

[a] Average of two XPS measurements at different spots. [b] Bi/Mo ratio in the bulk determined by ICP-OES equals 1.9. [c] Test conditions: $C_3H_6/O_2/N_2$ = 5/25/70, total flow of 50 Nml/min, 500 mg catalyst.

The samples synthesized with Bi/Mo = 1:1 and Bi/Mo = 2:3 exhibited similar surface areas (19 m²/g and 18 m²/g respectively, cf. Table 1). The sample synthesized with an excess of bismuth (Bi/Mo = 2:1) exhibited the highest surface area (45 m²/g). Whereas the spherical particles of this sample were approximately 25 nm in size (see TEM images in Fig. S3 a-b, ESI †), the samples with initial Bi/Mo ratio of 1:1 and 2:3 yielded larger particles with smaller spherical particles with a diameter < 10 nm on top (Fig. S3 d-f, ESI †). In line with the objective of the work, the surface areas were higher compared to other unsupported bismuth molybdates previously tested in the selective oxidation of propylene.

The β-phase is only considered stable at temperatures between 540 and 665 °C [17] and, thus, FSP represents a valuable technique to prepare this metastable high-temperature phase with high surface area for catalysis. In a similar way, Kemmler et al. [27] recently used this approach for the synthesis of the high temperature phase $In_4Sn_3O_4$, which showed excellent performance in sensor applications and long-term stability at the operation conditions.

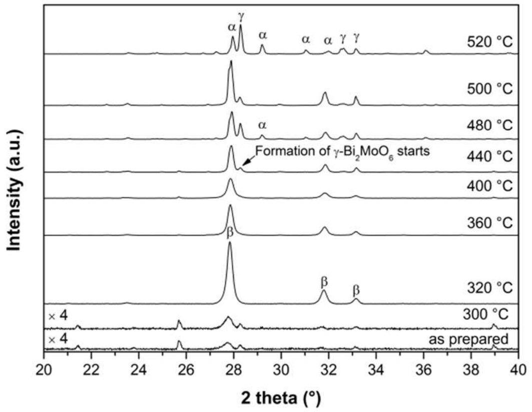

Fig. 2 PXRD analysis of the stability of flame made β-$Bi_2Mo_2O_9$ after calcination at different temperatures. The formation of γ-Bi_2MoO_6 from β-$Bi_2Mo_2O_9$ sets in at 440 °C. At 480 °C and 500 °C α-, β- and γ-phase were present, whereas at 520 °C β-$Bi_2Mo_2O_9$ was below the detection limit.

As the β-phase is a metastable phase, another proof of its existence is the instability below 540 °C. For this purpose, fresh samples were calcined at various temperatures for 4 h and analyzed by PXRD (Fig. 2). The formation of γ-Bi_2MoO_6 set in at 440 °C, as indicated by its characteristic reflection at 28.3° (see also patterns of the phase mixtures in ref. 28). The decomposition into α-$Bi_2Mo_3O_{12}$ and γ-Bi_2MoO_6 was completed at 520 °C, when no more β-bismuth molybdate could be detected by X-ray diffraction. Consequently, this also proves indirectly the existence of the β-phase. At the same time, the results demonstrate that the β-phase is stable at least during calcination under industrially relevant conditions. [3]

Hence, these flame-derived bismuth molybdates were applied in the selective oxidation of propylene using three different flows (50, 80 and 120 Nml/min) resulting in three different contact times (details see ESI †). In Fig. **3** the activity and selectivity of the different phases are depicted at 360 °C, which is close to the temperature used in industrial applications. Interestingly, β-$Bi_2Mo_2O_9$ showed the highest propylene conversion (15-28%), whereas α-$Bi_2Mo_3O_{12}$ exhibited the lowest propylene conversion (2-5%). γ-Bi_2MoO_6, which featured the highest specific surface area (45 m²/g), did not lead to the highest propylene conversion (9-15%). Acrolein selectivity remained stable around 70-80% with increasing propylene conversion (c.f. Fig. **3**b). The higher surface area of γ-Bi_2MoO_6 did not increase the amount of CO_x. Temperature-dependent catalytic activity measurements showed that the β-phase was also more active at 400 and still at 440 °C (cf. Fig. S4, ESI †), where its decomposition started. The used samples were characterized by PXRD (Fig. S5, ESI †) and XAS (Fig. S6, ESI †). Both analysis methods revealed that the β-phase decomposed, while the samples synthesized with Bi/Mo = 2:1 (γ-Bi_2MoO_6) and 2:3 (α-$Bi_2Mo_3O_{12}$) did not change phase during the tests at higher temperatures.

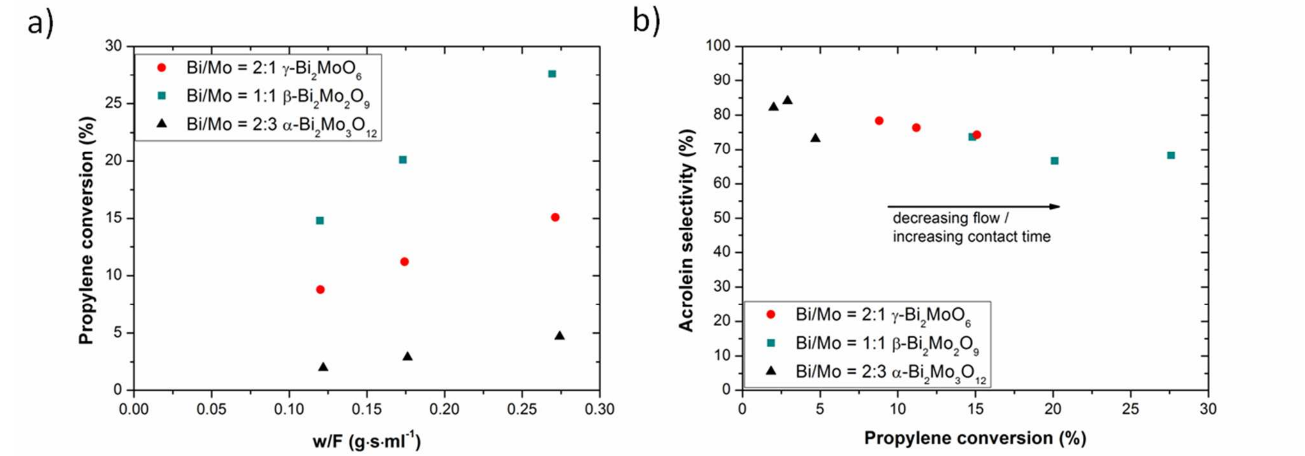

Fig. 3 Performance of the flame made materials in selective oxidation of propylene to acrolein at 360 °C (total flows: 50, 80 and 120 Nml/min; $C_3H_6/O_2/N_2$ = 5/25/70; 500 mg catalyst). a) Propylene conversion as a function of contact time (w/F; at measured reactor temperature and pressure) b) Acrolein selectivity as a function of propylene conversion.

Conclusions

In summary, flame spray pyrolysis gave access to three different bismuth molybdate phases (α-$Bi_2Mo_3O_{12}$, β-$Bi_2Mo_2O_9$ and γ-Bi_2MoO_6) with high surface area by variation of the Bi/Mo ratio. In particular, the method gave direct access to the high temperature metastable phase β-$Bi_2Mo_2O_9$. The activity of the different bismuth molybdate phases prepared by flame spray pyrolysis decreased in the following order: β > γ > α. In general, this selective one-step synthetic access to the Bi-Mo-O_x system nicely illustrates the great potential of flame spray pyrolysis for catalyst synthesis, in particular if high temperature phases such as the metastable β-$Bi_2Mo_2O_9$ need to be prepared.

This work was funded by the Danish Council of Strategic Research in the framework of the DSF proposal "Nanoparticle synthesis for catalysis". The European Synchrotron Radiation Facility (ESRF) in Grenoble is acknowledged for providing XAS beamtime at the beamline BM01B.

Notes and references

[a] Karlsruhe Institute of Technology (KIT), Institute of Chemical Technology and Polymer Chemistry (ITCP), Engesserstr. 20, 76131 Karlsruhe (Germany). E-Mail: grunwaldt@kit.edu

[b] Institute of Catalysis Research and Technology (IKFT), Hermann-von-Helmholtz-Platz 1, Building 725, 76344 Eggenstein-Leopoldshafen (Germany).

[c] Technical University of Denmark (DTU), Department of Chemical Engineering & Biochemical Engineering, Søltofts Plads Building 229, DK-2800 Kgs. Lyngby (Denmark).

[d] Karlsruhe Institute of Technology (KIT), Institute of Applied Materials (IAM) and Karlsruhe Nano Micro Facility (KNMF), Hermann-von-Helmholtz-Platz 1, 76344 Eggenstein-Leopoldshafen (Germany).

† Electronic Supplementary Information (ESI) available: Materials and methods; supplementary text; Fig. S1 – S6. See DOI: 10.1039/c000000x/

1 E. Pierson, M. Giella and M. Tishler, *J. Am. Chem. Soc.*, 1948, **70**, 1450.
2 Y. Oda, K. Uchida and T. Morimoto, U.S. Patent 3,865,873, 1975.
3 Y. Morooka and W. Ueda, *Adv. Catal.*, 1994, **40**, 233.
4 D. H. He, W. Ueda and Y. Morooka, *Catal. Lett.*, 1992, **12**, 35.
5 D. Carson, G. Coudurier, M. Forissier, J. C. Védrine, A. Laarif and F. Theobald, *J. Chem. Soc., Faraday Trans. 1*, 1983, **79**, 1921.
6 Z. Bing, S. Pei, S. Shishan and G. Xiexian, *J. Chem. Soc., Faraday Trans.*, 1990, **86**, 3145.
7 M. T. Le, J. Van Craenenbroeck, I. Van Driessche and S. Hoste, *Appl. Catal., A*, 2003, **249**, 355.
8 G. I. Aleshina, C. Joshi, D. V. Tarasova, G. N. Kustova and T. A. Nikoro, *React. Kinet. Catal. Lett.*, 1984, **26**, 203.
9 I. Matsuura, R. Schut and K. Hirakawa, *J. Catal.*, 1980, **63**, 152.
10 C. Zhao and I. E. Wachs, *J. Phys. Chem. C*, 2008, **112**, 11363.
11 W. Ueda, Y. Morooka, T. Ikawa and I. Matsuura, *Chem. Lett.*, 1982, 1365.
12 A. M. Beale and G. Sankar, *Chem. Mater.*, 2003, **15**, 146.
13 M. T. Le, W. J. M. Van Well, I. Van Driessche and S. Hoste, *Appl. Catal., A*, 2004, **267**, 227.
14 A. Nell, A. B. Getsoian, S. Werner, L. Kiwi-Minsker and A. T. Bell, *Langmuir*, 2014, **30**, 873.
15 L. D. Krenzke and G. W. Keulks, *J. Catal.*, 1980, **64**, 295.
16 R. P. Rastogi, A. K. Singh and C. S. Shukla, *J. Solid State Chem.*, 1982, **42**, 136.
17 M. Egashira, K. Matsuo, S. Kagawa and T. Seiyama, *J. Catal.*, 1979, **58**, 409.
18 K. Schuh, W. Kleist, M. Høj, V. Trouillet, P. Beato, A. D. Jensen, G. R. Patzke and J.-D. Grunwaldt, *Appl. Catal., A*, 2014, **482**, 145.
19 A. J. Gröhn, S. E. Pratsinis and K. Wegner, *Chem. Eng. J.*, 2012, **191**, 491.
20 M. Høj, K. Linde, T. K. Hansen, M. Brorson, A. D. Jensen and J.-D. Grunwaldt, *Appl. Catal., A*, 2011, **397**, 201.
21 W. Y. Teoh, R. Amal and L. Mädler, *Nanoscale*, 2010, **2**, 1324.
22 H. K. Kammler, L. Mädler and S. E. Pratsinis, *Chem. Eng. Technol.*, 2001, **24**, 583.
23 L. Mädler, H. K. Kammler, R. Müller and S. E. Pratsinis, *J. Aerosol Sci.*, 2002, **33**, 369.
24 W. J. Stark, S. E. Pratsinis and A. Baiker, *Chimia*, 2002, **56**, 485.
25 J.-D. Grunwaldt, M. D. Wildberger, T. Mallat and A. Baiker, *J. Catal.*, 1998, **177**, 53.
26 A. P. V. Soares, L. D. Dimitrov, M. de Oliveira, L. Hilaire, M. F. Portela and R. K. Grasselli, *Appl. Catal., A*, 2003, **253**, 191.
27 J. A. Kemmler, S. Pokhrel, J. Birkenstock, M. Schowalter, A. Rosenauer, N. Barsan, U. Weimar and L. Mädler, *Sens. Actuators, B*, 2012, **161**, 740.
28 L.M. Thang, L.H. Bac, I. Van Driessche, S. Hoste, W.J.M. Van Well, Catal. Today, 2008, **131** (2008) 566.